THE JOURNAL OF PHYSICAL CHEMISTRY C

pubs.acs.org/JPCC Article

Hole Polaron Transport in Bismuth Vanadate $BiVO_4$ from Hybrid Density Functional Theory

Taifeng Liu,* Mengsi Cui, and Michel Dupuis*

Cite This: https://dx.doi.org/10.1021/acs.jpcc.0c07408 Read Online

ACCESS | Metrics & More | Article Recommendations | Supporting Information

ABSTRACT: We address here the chemical character and the mobility of hole polarons in $BiVO_4$ (BVO). Two distinct structures for hole polarons in BVO have been reported in the literature to date. "Standard" hybrid density functional theory (DFT) calculations have predicted hole polarons to be (BiO_8) dodecahedron-centered polarons, while Hubbard *U*-DFT (DFT + *U*) calculations have predicted single oxygen atom-centered polarons. Resolving these contrasting findings is critical to validate theory in materials research. We investigated the structure of hole polarons in BVO using hybrid DFT with varying fractions (α) of the exact exchange interaction that enters hybrid functionals. For values of the fraction α, from $\alpha = 0.25$ to $\alpha = 0.45$, we obtained both structures, the $h^+(BiO_8)$ hole structure and the $h^+(O)$ hole structure. For the smaller values of α, the $h^+(BiO_8)$ structure is lower in energy, while for the larger values of α, the $h^+(O)$ structure is more stable. The piece-wise linearity of DFT energies $E(q)$ with respect to a point defect charge q is maintained satisfactorily in all cases, although the deviation is the smallest for hybrid DFT with a small exact exchange fraction. For $\alpha = 0.25$, we determined the diffusivity of $h^+(BiO_8)$ holes from the Marcus/Holstein two-state model. The activation barrier for Bi-to-Bi hops ($\Delta G^{\#} \sim 76$ meV) and mobility ($\mu \sim 0.029$ cm^2 V^{-1} s^{-1}) are found to be in close agreement with the published THz experimental data ($\Delta G^{\#} \sim 90$ meV and $\mu_{exp} \sim 0.02$ cm^2 V^{-1} s^{-1}, respectively). In $h^+(BiO_8)$ structures, nearly 25% of the hole charge and unpaired spin reside on the Bi atom and the rest is divided among the eight O atoms. The hole is best described as a Bi-centered hole, rather than a Bi 6s hole. In contrast, in $h^+(O)$ structures, about 75% of the unpaired spin population resides on the O atom. These findings suggest that if one wishes to resolve this theoretical dichotomy, there remains a need for further experimental characterization of hole polarons in BVO with techniques that could identify the oxidation state of Bi and O atoms in operando conditions and help validate theoretical results of structure and transport.

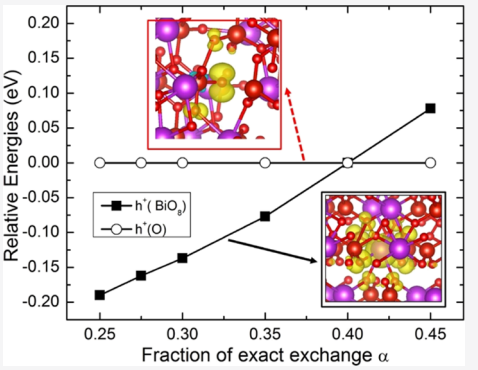

Downloaded via UNIV OF NEW ENGLAND on October 18, 2020 at 18:43:36 (UTC).
See https://pubs.acs.org/sharingguidelines for options on how to legitimately share published articles.

1. INTRODUCTION

Bismuth vanadate $BiVO_4$ (denoted BVO) is a promising semiconductor for photocatalytic or photoelectrochemical water splitting. Both electron and hole polarons have been observed. Rettie et al.[1,2] demonstrated that a small polaron hopping conduction mechanism dominates from 250 to 400 K in BVO. Abdi et al.[3] et al. measured the carrier mobility to be $\sim 4 \times 10^{-2}$ cm^2 V^{-1} s^{-1} by time-resolved microwave conductivity. Ziwritsch et al.[4] provided the first direct time-resolved evidence of hole polaron formation using THz spectroscopy, and they found the mobility of the self-trapped carrier to be ~ 0.02 cm^2 V^{-1} s^{-1}, which corresponds to a thermal hopping activation energy of ~ 90 meV. In experiments, it is difficult to separate electron and hole signals. Theoretical calculations have the potential to provide detailed information about the electronic/polaronic structure of electron or hole carriers, in particular, their "localized" characteristics and their mobilities.

Localization of the electron density and lattice relaxation are the quintessential electronic structure characteristics of electron/hole polarons, be they small or large polarons.[5−11] Density functional theory (DFT) has the potential to provide "exact" structures and energetics of these quantum species.[12,13] In the absence of the "exact" functional, we are left to choose a functional of the density that has deficiencies, from local density approximations (LDA) to generalized gradient approximations (GGAs), to hybrid functionals, to augmented density Hamiltonians. The self-interaction of unpaired electrons is one of the known deficiencies of functionals used to date that hybrid functionals[14,15] and augmented density Hamiltonians[16] attempt to correct.

In the case at hand of polarons in BVO, there is a general concurrence[17−23] that electron carriers are localized on vanadium atoms in BVO and form small polarons. The theories used span hybrid DFT[13,24−26] and DFT with Hubbard interaction terms DFT + *U*.[16,27,28] For hole carriers in BVO,

Received: August 13, 2020
Revised: September 21, 2020
Published: September 21, 2020

© XXXX American Chemical Society

there are very notable differences across theories. Using hybrid DFT (with HSE06 functional[29,30] with 25% fraction of the exact exchange interaction), Kweon[31,32] and Hwang reported that the excess hole charge spreads over one BiO_8 dodecahedron or across many Bi and O atoms, depending on the BVO phase. Using the hybrid PBE0 functional[33] with α = 0.22 fraction of the exact exchange interaction and molecular dynamics (MD) simulations, Wiktor[18] et al. found that the hole charge is distributed between one bismuth and eight oxygen atoms, and in about 20% of the MD configurations, the hole appears localized on a single oxygen atom. The hole structure exhibits a Bi−O bond shortening of ∼0.06 Å. In that work, the authors made use of new hybrid functionals that yield accurate band gaps while being able to describe polaronic distortions.[34,35]

In contrast to hybrid DFT, Pasumarthi[22] et al. and Liu[23] et al. used a DFT + U level of theory[16,27,28] with U_{eff} = 9 eV and found that an excess hole strongly localizes on a single oxygen atom. The optimized structure exhibits a Bi−O bond lengthening in the range of ∼0.12 to ∼0.18 Å. Liu[23] et al. verified that DFT + U with U_{eff} = 9 eV satisfies satisfactorily the behavior of the piece-wise linearity of DFT energies with respect to fractional occupation numbers, as it should. A number of other groups used similar values of $+U_{eff}$ to characterize holes in oxides.[36,37]

It is clear then that hybrid DFT and DFT + U lead to drastically different chemical descriptions of hole polarons in BVO. It is critically important to resolve the discrepancy. Both approaches correct in part for the self-interaction error of the LDA or GGA functionals. Both are ad hoc as users have the ability to select the value of the fraction α of the exact exchange interaction in hybrid DFT and of the $+U_{eff}$ value in DFT + U.

The goodness of mixing the exact exchange operator into local and non-local functionals of the density as a means to correct approximately for the self-interaction error of DFT is well-known and accepted. Early "standard" values of the mixing parameter (around ∼0.20 or ∼0.25) were adopted as the best compromise for molecular thermochemical data. The impact on solid-state energy properties was first noted by Muscat et al.[38] who reported band gaps much improved with hybrid functionals over GGA DFT and in close accord with experiments. However, in recent studies, Hegner et al.,[25] Wang et al.,[26] and Smart et al.[39] adopted smaller mixing values (α = 0.10, α = 0.145, and α = 0.12, respectively) based on theoretical arguments. They obtained "better" band gaps for stoichiometric BVO and oxygen vacancy-reduced BVO, as well as better band gap and small polaron structure in Co_3O_4. Note that oxygen vacancies give rise to electron polarons in gap states. These recent papers did not attempt to quantify the diffusivity of these electron carriers in these systems.

As a counterpoint, when aiming to characterize kinetics with DFT via the determination of activation barriers (electron/hole polaron hopping falls in this category), Zhao et al.[40] demonstrated that a larger mixing value, α = 0.42, corrects more accurately the self-interaction error in transition-state structures. They proposed the BB1K functional as a "better" functional. Interestingly, To et al.[41] showed that the BB1K functional describes very well the electronic structure of the $[AlO_4]^0$ defects in silica. $[AlO_4]^0$ defects in silica are hole localized on single oxygen atoms adjacent to Al sites, in accord with spectroscopic measurements. This was in striking contrast to other functionals with smaller α values that yielded incorrect electronic structures of $[AlO_4]^0$ defects. The oxygen-localized hole structure of $[AlO_4]^0$ is relevant to the characterization of the structure and electronic structure of (oxygen) hole polarons in oxides and other transition-metal semiconductors. Thus, the work by To et al.[41] suggests that larger values of α may be more appropriate for (oxygen) hole polarons, albeit oxygen-localized holes in metal oxides may be different than in doped silica.

In this communication, we seek to assess the effect of the hybrid fraction parameter α on the localized character of hole polarons in BVO. We report calculations of holes in BVO using hybrid density functionals with varying fractions of the exact exchange interaction. By controlling the initial geometry, we generate for each value of α two distinct "optimized" structures. In one structure denoted $h^+(BiO_8)$, the hole is centered on a bismuth atom and reaches out to its eight neighbor oxygen atoms with the hole magnetic moment on Bi increasing slightly with α and in the range of ∼0.15 to 0.25. In the other structure denoted $h^+(O)$, the hole is localized on two oxygen atoms when α < 0.3 and on a single oxygen atom for larger values of α. The $h^+(BiO_8)$ structure is more stable than the $h^+(O)$ structure for small values of α. When α = 0.4, the energies of the two structures are essentially the same. When α > 0.4, the $h^+(O)$ structure is more stable than the $h^+(BiO_8)$ structure. For small values of α, the electronic structure of hole polarons in BVO from hybrid DFT is better described as a Bi-centered delocalized "hole" $h^+(BiO_8)$ species, not a Bi 6s hole. Nevertheless and interestingly, we found that the activation barrier for hopping of the $h^+(BiO_8)$ species obtained with hybrid DFT with α = 0.25, using the Marcus/Holstein two-state model of small polaron hopping in connection with Einstein's diffusion model, is $\Delta G^* \sim 76$ meV with a mobility ∼0.029 $cm^2\ V^{-1}\ s^{-1}$, which happens to be in good accord with Ziwritsch's experimental value ∼0.02 $cm^2\ V^{-1}\ s^{-1}$ and a barrier of ∼90 meV.

In the end, we are not able to resolve the dichotomy between the Bi-centered $h^+(BiO_8)$ electronic structure with its mobility in good accord with experimental hole mobility in BVO obtained with small values of α and the strongly oxygen-localized hole structure obtained with larger α values. This observation points to the need for further experimental characterization of hole polarons in BVO. In particular, spectroscopies that focus on the oxidation states of selected elements, such as ultrafast UV spectroscopy, would be very valuable.[42] The paper is organized as follows: we give the computational details in Section 2, present and discuss results in Section 3, and conclude in Section 4.

2. COMPUTATIONAL DETAILS

We carried out spin-polarized DFT calculations using the Vienna Ab initio Simulation Package (VASP) code[43,44] and adopted the Perdew−Burke−Ernzerhof (PBE) parametrization[45] of the exchange and correlation potential in the GGA.[46] The electronic wave functions were expanded in plane waves with an energy cutoff of 400 eV. We treated the O ($2s^2$,$2p^4$), V ($3p^6$,$4s^2$,$3d^3$), and Bi ($5d^{10}$, $6s^2$,$6p^3$) electrons as valence electrons, with the core electrons represented by projector-augmented-wave potentials. Self-consistent DFT energies were converged to 10^{-4} eV, and geometry optimizations were deemed converged when the residual forces on the atoms were smaller than 0.01 eV/Å. The cell parameters were taken from experiment (a = 5.196 Å, b = 11.705 Å, c = 5.094 Å, α = 90°, β = 90.38°, and γ = 90°), and the atomic positions within the

https://dx.doi.org/10.1021/acs.jpcc.0c07408
J. Phys. Chem. C XXXX, XXX, XXX−XXX

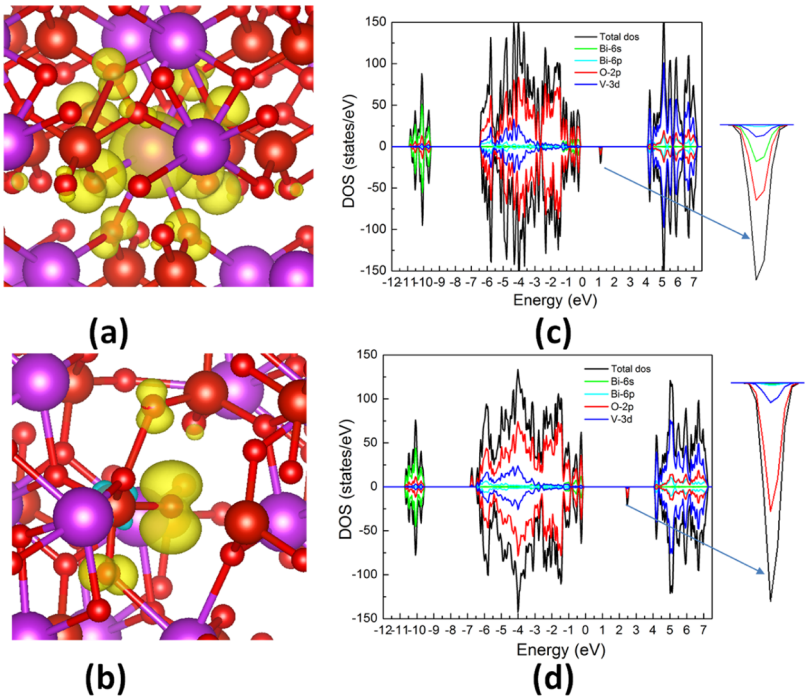

Figure 1. Spin density and DOSs for a hole localized on BiO_8 dodecahedra with $\alpha = 0.25$ and a single O atom when the fraction of exact exchange $\alpha = 0.4$. (a) Spin density of hole localized on a BiO_8 dodecahedron. (b) Spin density of a hole localized on one single O atom. Purple spheres are Bi atoms, larger red spheres are V atoms, and small red spheres are O atoms. (c) DOS for a hole localized on a BiO_8 dodecahedron. (d) DOS of a hole localized on one single O atom.

unit cell were optimized using a $5 \times 5 \times 2$ mesh of k-points. We used a $(2 \times 2 \times 1)$ supercell for the hole polaron calculations.

We used the HSE-based hybrid density functional,[47] for which the exchange and correction energy has the form

$$E_{XC}^{HSE} = \alpha E_X^{SR}(\mu) + (1-\alpha)E_X^{PBE,SR}(\mu) + E_X^{PBE,LR}(\mu) + E_C^{PBE} \quad (1)$$

where α and μ are the fraction of exact exchange interaction and the screening parameter, respectively. Here, we used $\alpha = 0.25, 0.275, 0.3, 0.35, 0.4$, and 0.45, successively, and $\mu = 0.207$ for the screening parameter, a value that has been shown to be a reasonable compromise between accuracy and computational cost.[48] For HSE geometry optimizations, we used the single Γ k-point approximation. Hole polarons were modeled by removing an electron from the system. To generate initial guesses as localized small polaron structures of holes, we resorted to a number of "techniques" (sometimes a combination of them) to create an initial density whereby the hole was localized predominantly on a single atom (a bismuth atom or an oxygen atom for hole polarons). In some instances, we lengthened the bonds around the site of localization by ~0.2 Å. Electron and spin densities were analyzed via the "atoms in molecules" analysis of Bader.[49]

In light of the fact that we obtained two distinct structures (see below) for hole polarons for any single value of the fraction α of exact exchange in the DFT energy, we evaluated the piece-wise linearity of the DFT energy $E(q)$ with respect to a charge q, where $q = 0.0$ to $+1.0$ is the amount of partial charge removed from the total density. This assessment follows closely the discussion by Lany and Zunger.[50] We had carried the same assessment for our DFT + U calculations in our earlier work.[23] We chose $\alpha = 0.25$ and 0.4 for these calculations. The results are shown in Figure S1 and Table S3 in the Supporting Information. It can be seen there that the energy deviations for $E(q)$ versus q do not exhibit strongly undesirable deviation from piece-wise linearity of the DFT energy as a function of positive-charge magnitude for either of the hole polaron structures and for the two values of α. The DFT + U results are included as well for ease of comparison. We view the assessment as being un-conclusive, albeit the smallest piece-wise linearity deviations are smallest for $\alpha = 0.25$.

3. RESULTS AND DISCUSSION

3.1. Hole Polaron Structures, Energies, and Stability.

For each value of the fraction α, we determined two structures as local minima on the potential energy surface of the total system. We denote them $h^+(BiO_8)$ and $h^+(O)$. They are highlighted in Figure 1 through a display of spin density contours as well as projected density of states (PDOS). The corresponding POSCAR files for VASP for HSE ($\alpha = 0.25$) are given in the Supporting Information.

As mentioned earlier, it is well known that LDA and GGA functionals of the density in DFT often fail to yield localization of unpaired spins due to their inherent self-interaction error. Partial mixing of the exact exchange interaction functionals is a means to correct in part for the self-interaction error. With increasing α, the unpaired spin becomes more and more "localized".

3.1.1. $h^+(BiO_8)$ and $h^+(O)$ Structures. Isodensity surfaces of the spin density as well as PDOS are useful in visualizing and contrasting the $h^+(BiO_8)$ and $h^+(O)$ structures. They are displayed in Figure 1 for hole on (BiO_8) with $\alpha = 0.25$ and hole on single oxygen atom with $\alpha = 0.4$. Figure 1a shows the $h^+(BiO_8)$ hole "centered" on one Bi and the neighbor oxygen atoms of a BiO_8 dodecahedron. This picture is similar to the

https://dx.doi.org/10.1021/acs.jpcc.0c07408
J. Phys. Chem. C XXXX, XXX, XXX−XXX

Table 1. Magnetic Moment Distribution for $h^+(BiO_8)$ and $h^+(O)$ for Different Values of the Fraction of Exact Exchange α[a]

	$h^+(BiO_8)$	$h^+(O)$	ΔE (eV)
fraction of exact exchange α	magmom(Bi)/magmom[$h^+(BiO_8)$]	magmom(O1):magmom(O2)/magmom[$h^+(O)$]	$E[h^+(O)] - E[h^+(BiO_8)]$
0.250	0.1692/0.9474	0.4261: 0.4312/0.8713	0.190
0.275	0.1813/0.9491	0.4722: 0.3965/0.8683	0.162
0.300	0.1946/0.9593	0.5752: 0.2954/0.8697	0.137
0.350	0.2152/0.9701	0.7072: 0.1104/0.8435	0.077
0.400	0.2356/0.9792	0.7292: 0.1247/0.8362	0.000
0.450	0.2523/0.9881	0.7416: 0.1312/0.8337	−0.078

[a]O1 and O2 refer to the two oxygen sites involved in $h^+(O)$ for small values of α; for larger values of α, $h^+(O)$ becomes localized on a single oxygen site. ΔE (4th column) is the relative energy of $h^+(BiO_8)$ and $h^+(O)$.

picture in Wiktor[18] et al. albeit their picture was obtained with α = 0.22. Figure 1b shows clearly an $h^+(O)$ localized polaron.

The PDOS in Figure 1c,d show a notable shift in the position of the gap state (arising from the hole state) between the two hole polaron structures. We note that the peak for the gap state for $h^+(BiO_8)$ (Figure 1c) exhibits a large contribution from O 2p and a small contribution from the Bi 6s atomic state with the Bi 6s state residing, by in large, at ∼10 eV below the top of the valence band that is made up of O 2p states. This is consistent with the magnetization shown in Table 1, with only ∼20% of the spin density localized on the Bi atom and the rest distributed among the O atoms. For $h^+(O)$, as seen in Figure 1d, the gap state shows essentially no contribution from the Bi 6s or Bi 6p states. The hole is localized on a single O atom. The corresponding PDOS in Figure 1d shows a gap state with mainly contribution from O 2p, and no Bi 6s contribution.

Bond length data for $h^+(BiO_8)$ and $h^+(O)$ for α = 0.25 and α = 0.40 are summarized in Table S1 in the Supporting Information where they are also contrasted with the bond lengths in stoichiometric BVO. From Table S1, it can be seen that when the hole is localized on a (BiO_8) unit, several Bi−O bonds have increased lengths by ∼0.03 Å. Other Bi−O bonds have shorter lengths by up to ∼0.07 Å. We note also that in these $h^+(BiO_8)$ structures, the symmetry of the (BiO_8) dodecahedra remains. The hole is centered around the Bi site and spreads over the (BiO_8) unit. (We will see below that less than 20% of the unpaired spin resides on the Bi atom, and the rest is divided across the eight oxygen atoms.) When the hole localizes on one single oxygen atom as in $h^+(O)$, the length of the Bi−O bond become longer by ∼0.2 Å, and the length of the O−V bond becomes also longer by ∼0.04 Å. (In these cases, a large fraction of the unpaired spin resides on the single oxygen site, and the hole is localized on a single O atom.) The bond length changes in $h^+(BiO_8)$ are much smaller compared to those in the $h^+(O)$ structure with localization on one single atom most likely because the lattice relaxation energy associated with the polaron is "absorbed" over eight bonds.

3.1.2. $h^+(BiO_8)$ and $h^+(O)$ Charges and Spins as a Function of α. Charge and spin populations are useful descriptors of the electronic structure of the $h^+(BiO_8)$ and $h^+(O)$ species. With regard to charge populations, the total Bader charge populations (spin up + spin down populations) are shown in the Supporting Information in Table S2 for the units defining the polaron structures as a function of α. In stoichiometric BVO, Bi atoms carry a positive charge ∼+2.17, while O atoms carry a negative charge ∼−1.15 when α = 0.25. The charges increase slightly in magnitude as α increases. The positive charge of the hole polaron amounts to ∼+0.56 on $h^+(BiO_8)$, ∼+0.12 coming from Bi and ∼+0.44 from the eight O's, while it is ∼+0.54 for $h^+(O)$. These values become ∼+0.86 (∼+0.20 and ∼+0.66) and ∼+0.78, respectively, when α = 0.45. Thus, the contribution of Bi to the hole polaron $h^+(BiO_8)$ amounts to a small amount of ∼+0.12 of one electron when α = 0.25. The contributions of the O's to the hole charge in $h^+(BiO_8)$ amounts to almost 4 times as much as the Bi contribution.

With regard to magnetic moments, they are given in Table 1. The magnetic moments ("magmom") on the polaronic atoms were extracted from the Bader charge density analysis (spin up minus spin down densities). For the $h^+(BiO8)$ structure, we give the "magmom" values for the Bi atom proper along with for the BiO_8 dodecahedron centered at the Bi atom. It is striking that the magmom of the hole is less than 20% localized on the Bi, and the rest is distributed among the eight oxygen atoms forming the BiO_8 dodecahedron. For the $h^+(O)$ structure, when α is smaller than ∼0.3, the $h^+(O)$ hole magmom is divided mostly between two oxygen atoms for the smaller values of α. Gradually, when α becomes larger than 0.35, the $h^+(O)$ hole magmom becomes localized on a single oxygen atom.

Overall, the total charge populations and the "magmom" populations point to $h^+(BiO_8)$ being better described as a Bi-centered hole rather than a Bi 6s hole. The oxidation state of Bi changes very little, and the hole may be viewed as a resonance of valence structures with the hole appearing delocalized over resonant Bi−O bonds.

3.1.3. $h^+(BiO_8)$ and $h^+(O)$ Relative Energies as a Function of α. For each value of α, we obtained two structures, one that we described as $h^+(BiO_8)$ and the other as $h^+(O)$. For each value of α, we can compare their DFT energies, while using the $h^+(O)$ energy as reference. We display in Figure 2 the relative energies of the $h^+(BiO_8)$ and $h^+(O)$ structures as we vary α. For values of α between ∼0.20 and ∼0.4, the $h^+(BiO_8)$ structure is more stable than the $h^+(O)$ structure. At α ∼0.4, the two structures have nearly the same energy. Above α ∼0.40, the $h^+(O)$ structure is more stable than the $h^+(BiO_8)$ structure. Recall that DFT + U does not yield a $h^+(BiO_8)$ structure; it yields only an $h^+(O)$ structure with spin localized on a single oxygen atom.

3.2. $h^+(BiO_8)$ Hopping Rates between Two BiO_8 Units as a Function of α. The $h^+(O)$ hole mobility has been fully characterized in previous publications.[22,23] Observing that $h^+(BiO_8)$ is significantly more stable than $h^+(O)$ for the smaller values of α, we decided to determine the $h^+(BiO_8)$ mobility for hopping across BiO_8 units as a function of α.

The methodology for calculation of activation barriers and mobility has been described in several publications.[51−55] We refer the reader to these papers. In brief, we use the two state Marcus/Holstein model of polaron hopping, whereby we

https://dx.doi.org/10.1021/acs.jpcc.0c07408
J. Phys. Chem. C XXXX, XXX, XXX−XXX

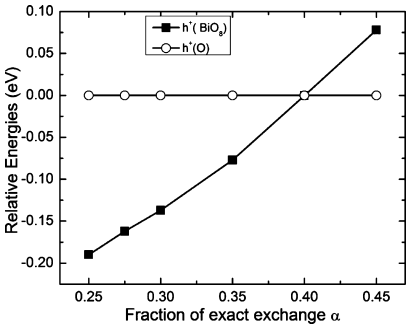

Figure 2. Relative energies of the two holes polaron structures $h^+(BiO_8)$ and $h^+(O)$ obtained with HSE(α) for each value of α when α varies from 0.25 to 0.40: square symbols are for the hole distributed over one Bi atom and the neighboring oxygen atoms, $h^+(BiO_8)$; the circle symbols are for the hole localized on two or one oxygen atom, $h^+(O)$.

determine two "localized" structures (the left or initial "0" structure and the right or final "1" structure) defined at the DFT level of theory. We define an approximate hopping pathway based on the initial and final structures and calculate the DFT energies along the reaction pathway, as depicted in Figure 3.

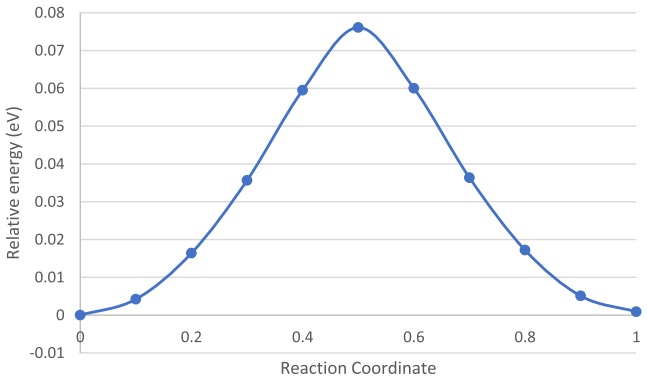

Figure 3. Energy curve for $h^+(BiO_8)$ hole hopping between two nearest Bi sites.

In our approach, the approximate pathway corresponds to a linear morphing of the initial and final structures. Analysis of the pathway indicates that it corresponds to a motion of the atoms along an anti-phase symmetric breathing phonon mode associated with the polaron sites.[51,56,57] (For reason of symmetry, the energies of point "0" and "1" are identical in BVO.) The transition state is at the mid-point 0.5 of the reaction coordinate. There are two general cases for the electronic structure at the mid-point: (1) the excess spin of the polaron hole could be "localized" to a significant extent on either the left or right site, indicating that the two polaron states are "quasi-diabatic" and hopping occurs via tunneling; (2) the excess spin of the polaron hole is split equally between the two sites, indicating that the energy curve is "adiabatic" in character, and hopping is a thermal process assisted by the phonon mode of the hopping pathway. In these cases, the "transition state" can be viewed as the state resulting from the superposition of two valence bond structures, and the top of the barrier arises from an avoided crossing of the two quasi-diabatic localized states.

Somewhat more extended approaches have been used for the characterization of the "transition state" at the top of the barrier.[58,59] A useful analysis can be found in the work of Adelstein et al.[58] who studied polaron hopping in Fe_2O_3 using the method of linear morphing as well as the "nudged elastic band" method[60] for the determination of reaction pathways. This study shows that the linear morphing approach is in semi-quantitative accord with the more sophisticated NEB approach. It establishes that the linear morphing approach is a reasonable approximation to the reaction pathway. That this is the case is due to the smallness of the distortions associated with the polarons. The good accord between computed and measured polaron drift mobilities obtained in the studies referenced above[51−55] further supports that the model is of good quality.

We calculated such curves for $h^+(BiO_8)$ transfer between adjacent Bi sites in BVO. The excess spin analysis discussed earlier indicates that the excess spin is split equally, and the process is "adiabatic".

The $h^+(BiO_8)$ mobility was determined from Einstein's equation

$$\kappa = i \times \upsilon_0 \, e^{-\Delta G^*/kT} \qquad D = \frac{R^2\kappa}{2} \qquad \mu = \frac{eD}{kT} \tag{2}$$

where κ is the hopping rate, ΔG^* is the activation energy, υ_0 is the frequency factor (taken as 10^{13} s^{-1}), i is a symmetry number for the number of equivalent hops for a given elementary pathway, here we take $i = 1$, D is the diffusion coefficient, and R is the site-to-site distance. The distance between two nearest Bi sites for $h^+(BiO_8)$ is ~3.901 Å, and μ is the mobility. $kT \sim 0.0256$ eV at $T = 298$ K. The determination of the pre-exponential frequency factor is discussed in several publications. See, for example, Adelstein et al.[58] and Oberhofer et al.[61] In their study of electron polaron hopping in Fe_2O_3, Adelstein et al.[58] showed that the value 10^{-13} s^{-1} of the frequency factor is reasonable. This is due to the fact that the phonon mode that induces the hopping process is a typical low-frequency metal oxide phonon mode in the range of ~0−800 cm^{-1}.

The energy at the top of the barrier ΔG^* was found to have a value of ~0.025, ~0.076, ~0.132, and ~0.187 eV when the mixing parameter had the value $\alpha = 0.15$, 0.25, 0.35, and 0.45, respectively. The corresponding mobilities are ~0.213, ~0.029, ~0.033, and ~0.038 10^{-2} cm^2 V^{-1} s^{-1}, respectively. That the activation barrier grows larger with increasing values of α is understandable. Large values of α favor stronger localization, so that the electron finds it more difficult to hop from one site to another. We note that in Ziwritsch's THz experiment, the measured mobility is ~0.02 cm^2 V^{-1} s^{-1}, corresponding to a hopping activation energy of ~90 meV. $\alpha = 0.25$ corresponds to the closest agreement with the experiment.

4. SUMMARY AND CONCLUSIONS

Before summarizing, it is interesting to reflect on the Bi 6s contribution to the gap state in the PDOS of the BiO_8-localized hole structure, as mentioned earlier. That result is consistent with the PDOS for stoichiometric BVO published by Walsh et al.[62] Yet the band at ~−10 eV comprises mostly Bi 6s. Hybridization of the 6s and 6p atomic states of Bi is therefore unexpected, given the energy gap of ~10 eV. In the Supporting Information of our earlier work,[23] we showed that the magnitude of s−p hybridization decreases in the

https://dx.doi.org/10.1021/acs.jpcc.0c07408
J. Phys. Chem. C XXXX, XXX, XXX−XXX

isoelectronic series N, P, As, Sb, and Bi, with a negligible amount of hybridization for Bi. Such an observation is consistent with the "inert pair effect" of Sidgwick[63] affecting Bi and making the Bi 6s electrons held tightly by the nucleus so that the Bi 6s level contributes very little to bonding. In light of this, it may not be appropriate to describe holes in BVO as "Bi 6s holes" but rather as Bi-center hole defects.

In summary, we investigated the structure of a hole polaron in BVO using hybrid DFT while varying the fraction α of the exact exchange interaction. For each value of α, from 0.25 to 0.45, we obtained two structures, one $h^+(BiO_8)$ with the hole residing within a BiO_8 dodecahedron and the other $h^+(O)$ with the hole localized on an oxygen atom. With the smaller values of α, the $h^+(BiO_8)$ structure is lower in energy, while for the larger values of α, the $h^+(O)$ structure is more stable. The $h^+(O)$ structures obtained with hybrid DFT are similar to the hole polaron structures obtained with DFT + U.

With α = 0.25, we characterized the energetics and kinetics of hole polaron transfer between two nearest neighbor (BiO_8) units using the Marcus/Holstein two-state model and determined the hole mobility from Einstein's theory of diffusion. The calculated activation energy and mobility are in close agreement with THz experimental data. Overall, we obtained contrasting structures when using hybrid DFT and DFT + U which suggest that additional spectroscopic characterization, for example, focused on oxidation states (e.g., ultrafast XUV spectroscopy or other), is needed to validate the theoretical data. The validation would establish broad and critical confidence in computational studies of carrier transport in transition-metal-based semiconductor photocatalysts.

■ ASSOCIATED CONTENT

Supporting Information

The Supporting Information is available free of charge at https://pubs.acs.org/doi/10.1021/acs.jpcc.0c07408.

CONTCAR files for $h^+(BiO_8)$ and $h^+(O)$ from HSE (α = 0.25) (ZIP)

Bond length data for hole polaron structures $h^+(BiO_8)$ and $h^+(O)$; Bader (spin up plus spin down) populations on h^+ polaron atoms; piece-wise linearity of energies E(q) with respect to defect charge q; and DFT data for the piece-wise linearity curves (PDF)

■ AUTHOR INFORMATION

Corresponding Authors

Taifeng Liu − *National & Local Joint Engineering Research Center for Applied Technology of Hybrid Nanomaterials, Henan University, Kaifeng 475004, China;* orcid.org/0000-0002-6869-7022; Email: tfliu@vip.henu.edu.cn

Michel Dupuis − *Department of Chemical and Biological Engineering, University at Buffalo, State University of New York, Buffalo, New York 14260, United States;* orcid.org/0000-0003-4799-3364; Email: mdupuis2@buffalo.edu

Author

Mengsi Cui − *Key Laboratory for Special Functional Materials of Ministry of Education, Collaborative Innovation Center of Nano Functional Materials and Applications, and School of Materials Science and Engineering, Henan University, Kaifeng, Henan 475001, China*

Complete contact information is available at: https://pubs.acs.org/10.1021/acs.jpcc.0c07408

Notes

The authors declare no competing financial interest.

■ ACKNOWLEDGMENTS

T. L. acknowledges support from the National Natural Science Foundation of China (grant # 21703054). M.D. acknowledges funds from the University at Buffalo and from the U.S. Department of Energy, Office of Science, Office of Basic Energy Sciences, under Award Number(s) DE-SC0019086 (interpretation of the data and writing of the manuscript).

■ REFERENCES

(1) Rettie, A. J. E.; Lee, H. C.; Marshall, L. G.; Lin, J.-F.; Capan, C.; Lindemuth, J.; McCloy, J. S.; Zhou, J.; Bard, A. J.; Mullins, C. B. Combined charge carrier transport and photoelectrochemical characterization of BiVO4 single crystals: intrinsic behavior of a complex metal oxide. *J. Am. Chem. Soc.* **2013**, *135*, 11389−11396.

(2) Rettie, A. J. E.; Chemelewski, W. D.; Lindemuth, J.; McCloy, J. S.; Marshall, L. G.; Zhou, J.; Emin, D.; Mullins, C. B. Anisotropic small-polaron hopping in W: BiVO4 single crystals. *Appl. Phys. Lett.* **2015**, *106*, 022106.

(3) Abdi, F. F.; Savenije, T. J.; May, M. M.; Dam, B.; van de Krol, R. The origin of slow carrier transport in BiVO4 thin film photoanodes: a time-resolved microwave conductivity study. *J. Phys. Chem. Lett.* **2013**, *4*, 2752−2757.

(4) Ziwritsch, M.; Müller, S.; Hempel, H.; Unold, T.; Abdi, F. F.; van de Krol, R.; Friedrich, D.; Eichberger, R. Direct time-resolved observation of carrier trapping and polaron conductivity in BiVO4. *ACS Energy Lett.* **2016**, *1*, 888−894.

(5) Rettie, A. J. E.; Chemelewski, W. D.; Emin, D.; Mullins, C. B. Unravelling Small-Polaron Transport in Metal Oxide Photoelectrodes. *J. Phys. Chem. Lett.* **2016**, *7*, 471−479.

(6) Emin, D. *Polarons*, 1st ed.; Cambridge University Press: New York, 2013.

(7) Emin, D.; Holstein, T. Studies of Small Polaron Motion. 4. Adiabatic Theory of Hall Effects. *Ann. Phys.* **1969**, *53*, 439−520.

(8) Emin, D. Correlated small-polaron hopping motion. *Phys. Rev. Lett.* **1970**, *25*, 1751−1755.

(9) Emin, D. Lattice relaxation and small-polaron hopping motion. *Phys. Rev. B: Solid State* **1971**, *4*, 3639−3651.

(10) Emin, D. Transport properties of small polarons. *J. Solid State Chem.* **1975**, *12*, 246−252.

(11) Emin, D.; Holstein, T. Adiabatic Theory of Hall Mobility of Small Polaron in Hopping Regime. *Bull. Am. Phys. Soc.* **1968**, *13*, 464.

(12) Hohenberg, P.; Kohn, W. Inhomogeneous electron gas. *Phys. Rev.* **1964**, *136*, B864−B871.

(13) Kohn, W.; Sham, L. J. Self-consistent equations including exchange and correlation effects. *Phys. Rev.* **1965**, *140*, A1133.

(14) Becke, A. D. A new mixing of hartree-fock and local density-functional theories. *J. Chem. Phys.* **1993**, *98*, 1372−1377.

(15) Becke, A. D. Density-functional thermochemistry . 3. The role of exact exchange. *J. Chem. Phys.* **1993**, *98*, 5648−5652.

(16) Anisimov, V. I.; Zaanen, J.; Andersen, O. K. Band theory and Mott insulators - Hubbard-U instead of Stoner-1. *Phys. Rev. B: Condens. Matter Mater. Phys.* **1991**, *44*, 943−954.

(17) Kweon, K. E.; Hwang, G. S.; Kim, J.; Kim, S.; Kim, S. Electron small polarons and their transport in bismuth vanadate: a first principles study. *Phys. Chem. Chem. Phys.* **2015**, *17*, 256−260.

(18) Wiktor, J.; Ambrosio, F.; Pasquarello, A. Role of Polarons in Water Splitting: The Case of BiVO4. *ACS Energy Lett.* **2018**, *3*, 1693−1697.

(19) Wu, F.; Ping, Y. Combining Landau−Zener theory and kinetic Monte Carlo sampling for small polaron mobility of doped BiVO 4 from first-principles. *J. Mater. Chem. A* **2018**, *6*, 20025−20036.

(20) Liu, T.; Zhou, X.; Dupuis, M.; Li, C. The nature of photogenerated charge separation among different crystal facets of BiVO 4 studied by density functional theory. *Phys. Chem. Chem. Phys.* **2015**, *17*, 23503−23510.
(21) Liu, T.; Pasumarthi, V.; LaPorte, C.; Feng, Z.; Li, Q.; Yang, J.; Li, C.; Dupuis, M. Bimodal hole transport in bulk BiVO 4 from computation. *J. Mater. Chem. A* **2018**, *6*, 3714−3723.
(22) Pasumarthi, V.; Liu, T.; Dupuis, M.; Li, C. Charge carrier transport dynamics in W/Mo-doped BiVO 4: first principles-based mesoscale characterization. *J. Mater. Chem. A* **2019**, *7*, 3054−3065.
(23) Liu, T.; Zhao, Q.; Li, C.; Lyu, Y.; Dupuis, M. Photocatalytic Facet Selectivity in BiVO4 Nanoparticles: Polaron Electronic Structure and Thermodynamic Stability Considerations for Photocatalysis. *J. Phys. Chem. C* **2019**, *123*, 20142−20151.
(24) Perdew, J. P.; Burke, K.; Ernzerhof, M. Generalized gradient approximation made simple (vol 77, pg 3865, 1996). *Phys. Rev. Lett.* **1997**, *78*, 1396.
(25) Hegner, F. S.; Forrer, D.; Galán-Mascarós, J. R.; López, N.; Selloni, A. Versatile Nature of Oxygen Vacancies in Bismuth Vanadate Bulk and (001) Surface. *J. Phys. Chem. Lett.* **2019**, *10*, 6672−6678.
(26) Wang, W.; Strohbeen, P. J.; Lee, D.; Zhou, C.; Kawasaki, J. K.; Choi, K.-S.; Liu, M.; Galli, G. The Role of Surface Oxygen Vacancies in BiVO4. *Chem. Mater.* **2020**, *32*, 2899−2909.
(27) Liechtenstein, A. I.; Anisimov, V. I.; Zaanen, J. Density-functional theory and strong-interactions - orbital ordering in mott-hubbard insulators. *Phys. Rev. B: Condens. Matter Mater. Phys.* **1995**, *52*, R5467−R5470.
(28) Dudarev, S. L.; Botton, G. A.; Savrasov, S. Y.; Humphreys, C. J.; Sutton, A. P. Electron-energy-loss spectra and the structural stability of nickel oxide: An LSDA+U study. *Phys. Rev. B: Condens. Matter Mater. Phys.* **1998**, *57*, 1505−1509.
(29) Heyd, J.; Scuseria, G. E.; Ernzerhof, M. Hybrid functionals based on a screened Coulomb potential. *J. Chem. Phys.* **2003**, *118*, 8207−8215.
(30) Heyd, J.; Scuseria, G. E. Hybrid functionals based on a screened Coulomb potential (vol 118, pg 8207, 2003). *J. Chem. Phys.* **2006**, *124*, 219906.
(31) Kweon, K. E.; Hwang, G. S. Surface structure and hole localization in bismuth vanadate: a first principles study. *Appl. Phys. Lett.* **2013**, *103*, 131603.
(32) Kweon, K. E.; Hwang, G. S. Structural phase-dependent hole localization and transport in bismuth vanadate. *Phys. Rev. B: Condens. Matter Mater. Phys.* **2013**, *87*, 205202.
(33) Perdew, J. P.; Ernzerhof, M.; Burke, K. Rationale for mixing exact exchange with density functional approximations. *J. Chem. Phys.* **1996**, *105*, 9982−9985.
(34) Miceli, G.; Chen, W.; Reshetnyak, I.; Pasquarello, A. Nonempirical hybrid functionals for band gaps and polaronic distortions in solids. *Phys. Rev. B* **2018**, *97*, 121112.
(35) Wiktor, J.; Reshetnyak, I.; Ambrosio, F.; Pasquarello, A. Comprehensive modeling of the band gap and absorption spectrum of BiVO4. *Phys. Rev. Mater.* **2017**, *1*, 022401.
(36) Herlihy, D. M.; Waegele, M. M.; Chen, X. H.; Pemmaraju, C. D.; Prendergast, D.; Cuk, T. Detecting the oxyl radical of photocatalytic water oxidation at an n-SrTiO3/aqueous interface through its subsurface vibration. *Nat. Chem.* **2016**, *8*, 556.
(37) Erhart, P.; Klein, A.; Åberg, D.; Sadigh, B. Efficacy of the DFT plus U formalism for modeling hole polarons in perovskite oxides. *Phys. Rev. B: Condens. Matter Mater. Phys.* **2014**, *90*, 035204.
(38) Muscat, J.; Wander, A.; Harrison, N. M. On the prediction of band gaps from hybrid functional theory. *Chem. Phys. Lett.* **2001**, *342*, 397−401.
(39) Smart, T. J.; Tuan Anh, P.; Ping, Y.; Ogitsu, T. Optical absorption induced by small polaron formation in transition metal oxides: The case of Co3O4. *Phys. Rev. Mater.* **2019**, *3*, 102401.
(40) Zhao, Y.; Lynch, B. J.; Truhlar, D. G. Development and assessment of a new hybrid density functional model for thermochemical kinetics. *J. Phys. Chem. A* **2004**, *108*, 2715−2719.
(41) To, J.; Sokol, A. A.; French, S. A.; Kaltsoyannis, N.; Catlow, C. R. A. Hole localization in AlO4 (0) defects in silica materials. *J. Chem. Phys.* **2005**, *122*, 144704.
(42) Biswas, S.; Husek, J.; Londo, S.; Baker, L. R. Highly Localized Charge Transfer Excitons in Metal Oxide Semiconductors. *Nano Lett.* **2018**, *18*, 1228−1233.
(43) Kresse, G.; Furthmüller, J. Efficient iterative schemes for ab initio total-energy calculations using a plane-wave basis set. *Phys. Rev. B: Condens. Matter Mater. Phys.* **1996**, *54*, 11169.
(44) Kresse, G.; Furthmüller, J. Efficiency of ab-initio total energy calculations for metals and semiconductors using a plane-wave basis set. *Comput. Mater. Sci.* **1996**, *6*, 15−50.
(45) Perdew, J. P.; Burke, K.; Ernzerhof, M. Generalized gradient approximation made simple. *Phys. Rev. Lett.* **1996**, *77*, 3865.
(46) Blöchl, P. E. Projector augmented-wave method. *Phys. Rev. B: Condens. Matter Mater. Phys.* **1994**, *50*, 17953.
(47) Heyd, J.; Scuseria, G. E.; Ernzerhof, M. Hybrid functionals based on a screened Coulomb potential. *J. Chem. Phys.* **2003**, *118*, 8207−8215.
(48) Schimka, L.; Harl, J.; Kresse, G. Improved hybrid functional for solids: The HSEsol functional. *J. Chem. Phys.* **2011**, *134*, 024116.
(49) Bader, R. F. W. *Atoms in Molecules—A Quantum Theory*; Oxford Universty Press: New York, 1990.
(50) Lany, S.; Zunger, A. Polaronic hole localization and multiple hole binding of acceptors in oxide wide-gap semiconductors. *Phys. Rev. B: Condens. Matter Mater. Phys.* **2009**, *80*, 085202.
(51) Rosso, K. M.; Smith, D. M. A.; Dupuis, M. An ab initio model of electron transport in hematite (α-Fe2O3) basal planes. *J. Chem. Phys.* **2003**, *118*, 6455−6466.
(52) Iordanova, N.; Dupuis, M.; Rosso, K. M. Charge transport in metal oxides: A theoretical study of hematite alpha-Fe2O3. *J. Chem. Phys.* **2005**, *122*, 144305.
(53) Deskins, N. A.; Dupuis, M. Electron transport via polaron hopping in bulk TiO2: A density functional theory characterization. *Phys. Rev. B: Condens. Matter Mater. Phys.* **2007**, *75*, 195212−195221.
(54) Deskins, N. A.; Dupuis, M. Intrinsic Hole Migration Rates in TiO2 from Density Functional Theory. *J. Phys. Chem. C* **2009**, *113*, 346−358.
(55) Liu, T.; Pasumarthi, V.; LaPorte, C.; Feng, Z.; Li, Q.; Yang, J.; Li, C.; Dupuis, M. Bimodal hole transport in bulk BiVO4 from computation. *J. Mater. Chem. A* **2018**, *6*, 3714−3723.
(56) Rosso, K. M.; Dupuis, M. Electron transfer in environmental systems: a frontier for theoretical chemistry. *Theor. Chem. Acc.* **2006**, *116*, 124−136.
(57) Rosso, K. M.; Dupuis, M. On charge transport in iron oxides. *Geochim. Cosmochim. Acta* **2005**, *69*, A778.
(58) Adelstein, N.; Neaton, J. B.; Asta, M.; De Jonghe, L. C. Density functional theory based calculation of small-polaron mobility in hematite. *Phys. Rev. B: Condens. Matter Mater. Phys.* **2014**, *89*, 245115−245123.
(59) Wu, F.; Ping, Y. Combining Landau-Zener theory and kinetic Monte Carlo sampling for small polaron mobility of doped BiVO4 from first-principles. *J. Mater. Chem. A* **2018**, *6*, 20025−20036.
(60) Henkelman, G.; Uberuaga, B. P.; Jónsson, H. A climbing image nudged elastic band method for finding saddle points and minimum energy paths. *J. Chem. Phys.* **2000**, *113*, 9901−9904.
(61) Oberhofer, H.; Reuter, K.; Blumberger, J. Charge Transport in Molecular Materials: An Assessment of Computational Methods. *Chem. Rev.* **2017**, *117*, 10319−10357.
(62) Walsh, A.; Yan, Y.; Huda, M. N.; Al-Jassim, M. M.; Wei, S.-H. Band Edge Electronic Structure of BiVO4: Elucidating the Role of the Bi s and V d Orbitals. *Chem. Mater.* **2009**, *21*, 547−551.
(63) Sidgwick, N. V. *The Electronic Structure of Valency*; Clarendon: Oxford, 1927; pp 178−181.

https://dx.doi.org/10.1021/acs.jpcc.0c07408
J. Phys. Chem. C XXXX, XXX, XXX−XXX